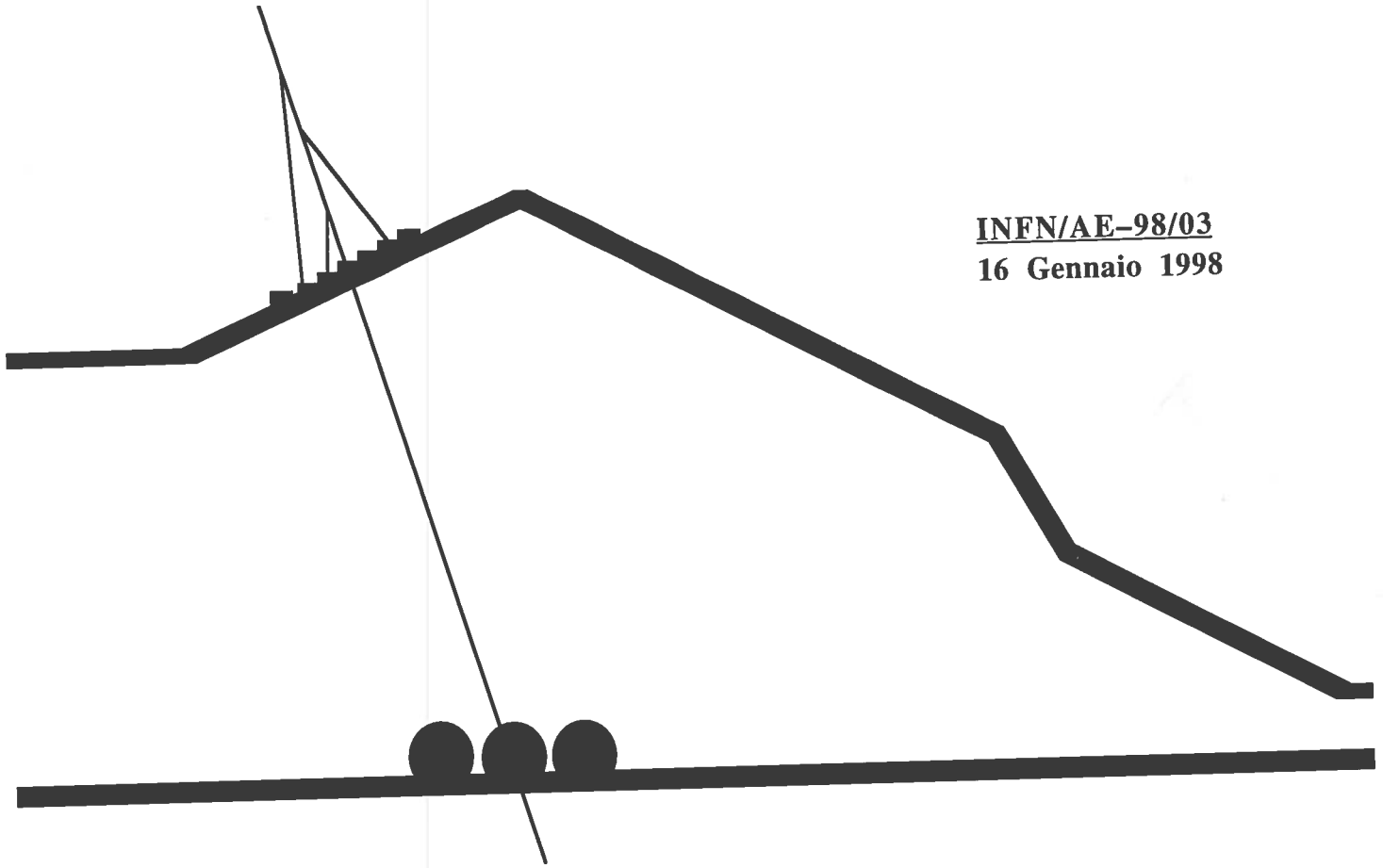

INFN/AE–98/03
16 Gennaio 1998

Simulation of Nuclear Effects in Quasi Elastic and Resonant Neutrino Interactions

G. Battistoni, P. Lipari, J. Ranft, E. Scapparone

INFN – Laboratori Nazionali del Gran Sasso

Published by ***SIS–Pubblicazioni***
dei Laboratori Nazionali di Frascati

INFN – Istituto Nazionale di Fisica Nucelare
Laboratori Nazionali del Gran Sasso

INFN/AE–98/03
16 Gennaio 1998

Simulation of Nuclear Effects in Quasi Elastic and Resonant Neutrino Interactions

G. Battistoni, P. Lipari, J. Ranft, E. Scapparone

Abstract

The effects of nuclear re-interactions in quasi elastic and resonant neutrino interactions have been considered in the framework of the nuclear models of the DPMJET code. A preliminary investigation on the modifications induced on the final state has been performed. Some consequences affecting the experimental identification are discussed.

1 Introduction

The interest in neutrino interaction is nowadays mostly oriented to the question of neutrino mass and flavour oscillations. The anomaly in atmospheric neutrino flux, pointed out by many experiments[1, 2, 3], suggested the possibility to explore the region $\Delta m^2 \simeq 10^{-2}$-$10^{-3}$ eV^2, using a Long Base Line (LBL) neutrino beam. Considering the recent CHOOZ result[4], ruling out the $\nu_\mu \rightarrow \nu_e$ explanation for the atmospheric anomaly, the interest for LBL experiments is shifted to ν_τ appearance search with energy $E_\nu \simeq$4–10 GeV, since the recent result from Superkamiokande[5], folded with the older Kamiokande and IMB results, suggests oscillation parameters $sin^2 2\theta \simeq 1$ and $\Delta m^2 \simeq 5{\cdot}10^{-3}$. The ν_τ tagging is rather difficult at these energies both from a statistical and an experimental point of view. The first point comes from the overlap of the low cross section at these energies with the poor neutrino flux in the LBL case, with respect to a Short Base Line situation, decreasing like $\simeq r^{-2}$, where r is the distance between the neutrino production point and the neutrino detection point. The second point is related to the intrinsic difficulties in measuring the kinematic variables of ν_τ interaction products at low energy.

However, at these neutrino energies, the selection of quasi elastic and resonant events can be useful to identify ν_τ candidates. At energies not far from the threshold for the production of τ lepton, the quasi elastic cross section gives still a large contribution to the the total charged current cross section. Moreover the intrinsic simplicity of the kinematics, simplifies the search "a la Nomad"[6] for ν_τ identification. Favourable are those events in which the τ lepton decays into an electron or muon (plus neutrinos) or into a single pion (plus neutrino).

However, the intrinsic cleanness offered by kinematics of the quasi–elastic interaction of neutrinos on single nucleons, can be obscured in case of nuclear targets. Nuclear effects, like Fermi motion and nuclear re–interaction of the nucleon inside the nucleus, have to be considered with care. These effects can provide momentum imbalance, the production of additional particles and may lead to the misidentification of the outgoing nucleon. All this phenomenology can deteriorate the signal/background ratio, the event recognition efficiency and the vertex identification. Moreover, in case of experiments that plan to use emulsions as active targets, one expects to see, sometimes, low energy particles and fragments close to the interaction vertex ("grey" and "black" particles, in the language of emulsions).

Guided by this consideration we start from the quasi–elastic and resonant neutrino scattering simulation code of [7], which already takes into account some nuclear effects, like Fermi motion and Pauli blocking. We have interfaced it to the

DPMJET-II-.4.1 code [8, 9, 10], which was created to treat hadron–nucleus and nucleus–nucleus interaction at high energy but which also contains a Formation Zone Intranuclear Cascade (FZIC) for low energy interaction of the produced secondaries with the spectator nucleons, nuclear evaporation and the formation of the residual nucleus. The nuclear models of DPMJET have been tested against a wide set of experimental data. In particular, the main check of the de–excitation and fragmentation algorithms comes from the comparison with emulsion data [11, 12].

More refined models which take into account the effect of the nuclear potential on the particle trajectories exist[13, 14, 15, 16, 17] and will be considered by other authors[18] also in the framework of neutrino simulation. While waiting for these more refined codes, we think that we can obtain from the use of DPMJET a lot of essential information, which, as a first approximation, is reasonable and not achievable from presently existing codes.

In this paper we present the first results obtained using this code, on the comparison with single nucleon interaction with and without considering the nuclear effects and the implication for ν_τ explicit search.

2 Description of the code

The code extends the quasi–elastic neutrino–nucleon and neutrino–nucleus model QEL[7], based on the formulation of Lewellyn–Smith[19], to neutrino collisions on nuclear targets including the intranuclear cascade and nuclear fragmentation and evaporation. The QEL code has been transformed to double precision, to match the DPMJET environment, and it has been modified to use the Fermi momenta of the nucleons from DPMJET.

All neutrino flavours can be considered. In the case of tau lepton production, the leptonic decay into muon (or electron) plus neutrinos can be optionally activated. For this reason, we have also introduced the calculation of the polarization of the final lepton, according to the treatment of [20].

The nucleon generated by the QEL code can re–interact in DPMJET inside the nucleus according to the Formation Zone Intranuclear Cascade (FZIC) model [21, 22, 11] contained inside DPMJET. Secondaries from this first collision are followed along straight trajectories and may induce in turn intranuclear cascade processes if they reach the end of their formation zone inside the target, otherwise they leave the nucleus without interaction. Inelastic secondary interactions in the FZIC are described by the Monte Carlo code HADRIN [23, 24]. For the sampling of elastic

nucleon–nucleon scattering below 4 GeV the parameterization of the HETC-KFA code [25, 26] was adopted.

The treatment of nuclear effects within the MC model has already been discussed in [27] and in more detail in [11, 12]. Since they are essential in calculating excitation energies of nuclei left after primary interactions and intranuclear cascade processes we summarize the basic ideas. Fermi momenta for nucleons as well as a simplified treatment of the nuclear potential are applied to control the generation of low–energy particles. Nucleon momenta are sampled from zero–temperature Fermi distributions

$$\frac{dN^{\mathrm{n,p}}}{dp} = N^{\mathrm{n,p}} \frac{3p^2}{(p_{\mathrm{F}}^{\mathrm{n,p}})^3}. \tag{1}$$

The maximum allowed Fermi momenta of neutrons and protons are

$$p_{\mathrm{F}}^{\mathrm{n,p}} = \left[\left(\frac{N^{\mathrm{n,p}}}{V_A} \right) \frac{3h^3}{8\pi} \right]^{\frac{1}{3}} \tag{2}$$

with V_A being the volume of the corresponding nucleus with an approximate nuclear radius $R_A = r_0 A^{1/3}, r_0 = 1.29$ fm.

Modifications of the actual nucleon momentum distribution, as they would arise, for instance, taking the reduced density and momenta in the nuclear skin into consideration, effectively result in a reduction of the Fermi momenta as compared to those sampled from Eq. (2). This effect can be estimated by a correction factor $\alpha_{\mathrm{mod}}^{\mathrm{F}}$ which modifies the Fermi–momenta. Results presented in this paper have been obtained with $\alpha_{\mathrm{mod}}^{\mathrm{F}}$=0.60. The depth of the nuclear potential is assumed to be the Fermi energy and the binding energy for outer shell nucleons

$$V^{\mathrm{n,p}} = \frac{(p_{\mathrm{F}}^{\mathrm{n,p}})^2}{2m_{\mathrm{n,p}}} + E_{\mathrm{bind}}^{\mathrm{n,p}}. \tag{3}$$

To extend the applicability of the model to the energy region well below 1 GeV an approximate treatment of the Coulomb–potential is provided. The Coulomb–barrier modifying the nuclear potential is calculated from

$$V_{\mathrm{C}} = \frac{e^2}{4\pi\epsilon_0 r_0} \frac{Z_1 Z_2}{(A_1^{1/3} + A_2^{1/3})} \tag{4}$$

with the mass numbers A_1, A_2 and charges Z_1, Z_2 of the colliding nuclei, i.e. with $A_1 = |Z_1| = 1$ for charged hadrons entering or leaving the target nucleus. e denotes the elementary charge and $r_0 = 1.29$ fm.

The excitation energy U of the residual nucleus with mass number $A_{\rm res}$ and charge $Z_{\rm res}$, i.e. the energy above the ground state mass $E_{0,\rm res}$, is given as

$$\begin{aligned} U &= E_{\rm res} - E_{0,\rm res}, \\ E_{0,\rm res} &= Z_{\rm res} m_{\rm p} + (A_{\rm res} - Z_{\rm res}) m_{\rm n} - E_{\rm bind}(A_{\rm res}, Z_{\rm res}). \end{aligned} \tag{5}$$

The binding energy $E_{\rm bind}(A_{\rm res}, Z_{\rm res})$ is obtained using the experimentally determined excess masses of all known (measured) nuclides and using mass formulae for nuclides far from the stable region, where no measurements are available. The excitation energy is obtained within our model from an explicit consideration of the effects of the nuclear potential (Eq. (3)) and the Coulomb energy (Eq. (4)), i.e. from corrections which are applied to the 4–momenta of the final state hadrons leaving the spectator nucleus. We modify the energies of these hadrons by the potential barrier and rescale the 3–momenta correspondingly. It is assumed that these corrections have to be applied to nucleons wounded in primary and secondary interactions and only to those hadrons which are formed inside the spectator nucleus corresponding to the sampled formation time. Among these particles we find apart from the nucleons a small fraction of other baryons, which are assumed to move in a nucleon potential and mesons to which we apply an effective meson potential of 0.002 GeV. Due to energy–momentum conservation these corrections lead to a recoil momentum and, therefore, to an excitation of the residual nucleus. In addition, there is a further contribution to the recoil momentum of the residual nucleus arising from potential corrections applied to the momentum of the projectile hadron entering the nuclear potential and from cascade nucleons with kinetic energies below the nuclear potential which are therefore not able to escape the spectator nucleus. Pauli blocking is considered, and events are rejected accordingly. Instead, no angular momentum barriers are considered.

At the end of the intranuclear cascade the residual nucleus is supposed to be left in an equilibrium state, in which the excitation energy U is shared by a large number of nucleons. Such an equilibrated prefragment nucleus is supposed to be characterized by its mass, charge, and excitation energy with no further memory of the steps which led to its formation. The excitation energy can be higher than the separation energy, thus nucleons and light fragments (α,d,^{3}H, ^{3}He) can still be emitted: they constitute the low–energy (and most abundant) part of the emitted particles in the rest system of the residual nucleus, having an average energy of few MeV.

In heavy nuclei the evaporative process is in competition with another equilibrium process, that is fission [28]. For the fission probability, a statistical method

can be used [29, 30].

Other de–excitation mechanisms are more suitable for light residual nuclei. The one adopted for this calculations is the so called Fermi Break–up model [31, 32], where the excited nucleus is supposed to disassemble just in one step into two or more fragments, with branching given by plain phase space considerations. According to the picture of the compound nucleus like an equilibrated system determined only by its mass, charge and excitation energy, with no memory of previous steps of the interaction, Fermi Break–up is activated in the model every time the current compound nucleus has mass number $A \leq 17$, including possible light fission fragments. The fragmentation of higher mass compound nuclei is not yet included in the model. This process, although its cross section is quite small, is important when considering the distribution of residual nuclei, because it can produce isotopes very far both from the target mass and from the fission product distribution.

The evaporation stage ends when the nuclear excitation energy becomes lower than all separation energies for nucleons and fragments. This residual excitation energy is then dissipated through emission of photons. γ–de–excitation proceeds through a cascade of consecutive photon emissions, until the ground state is reached. The cascade is assumed to be statistical as long as the excitation energy is high enough to allow the definition of a continuous nuclear level density. Below a (somewhat arbitrary) threshold, set at the pairing gap value, the cascade goes through transitions between discrete levels. In reality, photon emission occurs even during the preequilibrium and evaporation stages, in competition with particle emission, but its relative probability is low, and it is presently neglected in the model.

3 Simulation results

In order to test the features of the code, we considered 5,000 quasi elastic interactions of 10 GeV ν_μ on light (Carbon), intermediate (Silicon) and heavy (Iron) targets. We immediately see that additional particles appear in the final state. Table 1 shows the comparison of the results on different targets, as far as the average nucleon, gamma and charged pion multiplicities and the average de–excitation gamma energy are concerned. Moreover, we show the probability P to obtain a "clean" two body final state (just muon plus proton) and the average missing $P_\perp$. We notice that the main effect of the nuclear re–interaction consists in additional nucleon production, although at very low momentum, as it will be shown later. Charged pion production(whose kinetic energy is around 300 MeV) is rather negligible.

Target	$< N_{n,p} >$	$< N_{\pi\pm} >$	$< N_{\gamma} >$	$< E_{\gamma} >$ (MeV)	P(n=2)	$< P_{\perp}^{miss} >$ (MeV/c)
free nucleons	1.	0	0	0	100%	0
Carbon	1.49 $\pm$0.02	0.016 $\pm$0.002	0.79 $\pm$0.02	2.1	27.4%	175
Silicon	2.02 $\pm$0.02	0.025 $\pm$0.002	2.68 $\pm$0.02	1.5	0.%	183
Iron	2.26 $\pm$0.05	0.023 $\pm$0.005	3.42 $\pm$0.06	1.5	0.%	216

Table 1: *Comparison of the result of ν_{μ} interaction ($E_{\nu_{\mu}}$=10 GeV) on different targets.*

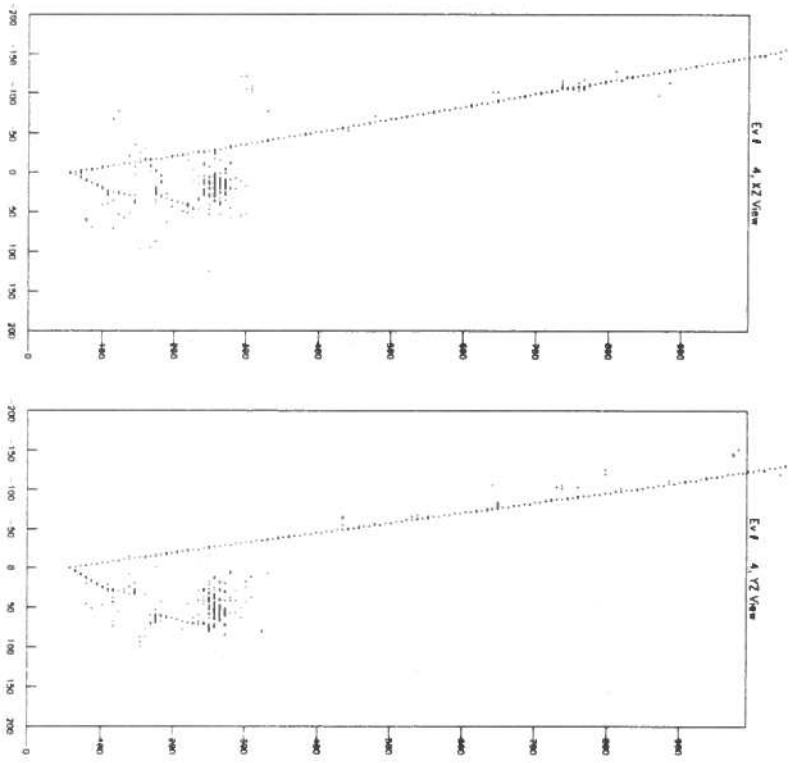

Figure 1: Example of a simulated quasi elastic ν_{μ} event at 10 GeV in a glass–scintillator sampling calorimeter (nuclear re–interaction off).

To give an idea of the event topology distortion introduced by nuclear effects, we simulated a fine grain low density sampling calorimeter (1/4 X_0 glass + 1.5 cm of liquid scintillator) using the FLUKA package[15]. Fig. 1 and 2 show the same QEL event, without nuclear effects (Fig. 1) and and with nuclear effects (Fig. 2). It's

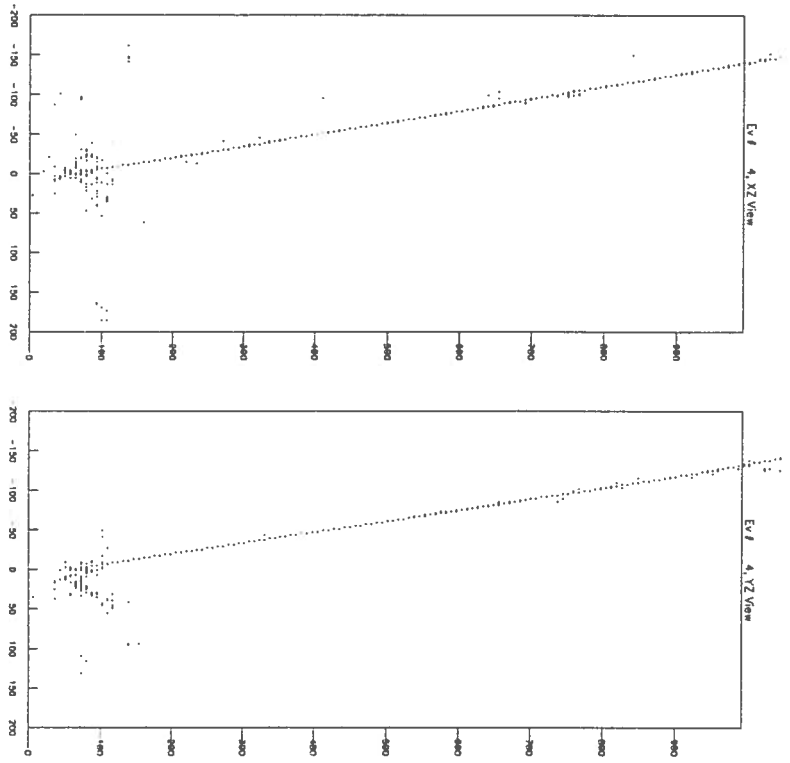

Figure 2: The same event of Fig. 1 when nuclear re–interactions are considered.

evident, looking at these figures, that the identification and tracking of the proton becomes more difficult, both for the presence of extra particle in the final state and for the modification of the kinematics of the proton itself.

Fig. 3 shows the momentum of the protons produced in the interaction. In the top part we consider all the protons emitted while in the bottom part, we considered only the event leading proton (the most energetic one). We show in the same figure the case with and without nuclear re–interaction. We learn that the bulk of the additional protons is produced with low momentum, as typical of intranuclear cascade products. As expected, the effect tends to become more significant for heavy

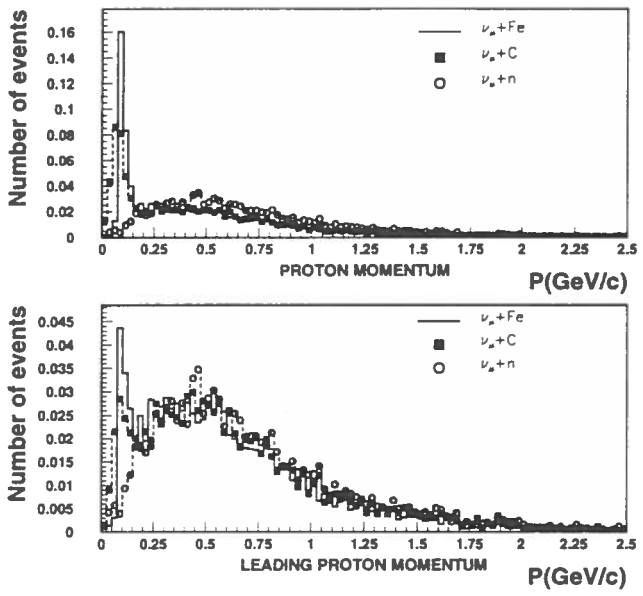

Figure 3: Protons (top) and leading proton(bottom) momentum distribution, in ν_μ+n, ν_μ+C and ν_μ+Fe interaction (E_{ν_μ} = 10 GeV)

target nuclei. There is also some dependence on energy. The effects of nuclear re–interaction manifest themselves in the distortion of the kinematic variables. As an example, in Fig. 4 we show the distribution of the angle between the muon and the outgoing leading proton. The case with and without nuclear re–interactions are distinguished and compared to the case of the free neutron target. We notice how the proton now, even the leading one, can access much larger angle with respect to the simple kinematics of pure neutrino–neutron quasi–elastic scattering. Further kinematic effect can be observed looking at event missing $P_\perp$. Also in naive models we expect the appearance of non zero missing $P_\perp$ from Fermi motion. Nuclear re–interactions increase this effect (Fig. 5 and 6 for C and Fe target respectively). There, we show in the top part the change in missing $P_\perp$ distribution from the case without intranuclear cascade (left) to the case including re–interactions (right). A tail in the last case is evident extending at large value of $P_\perp$; this is a dangerous effect for the experiments aiming to tag the ν_τ using kinematic cuts "a la Nomad"[6].

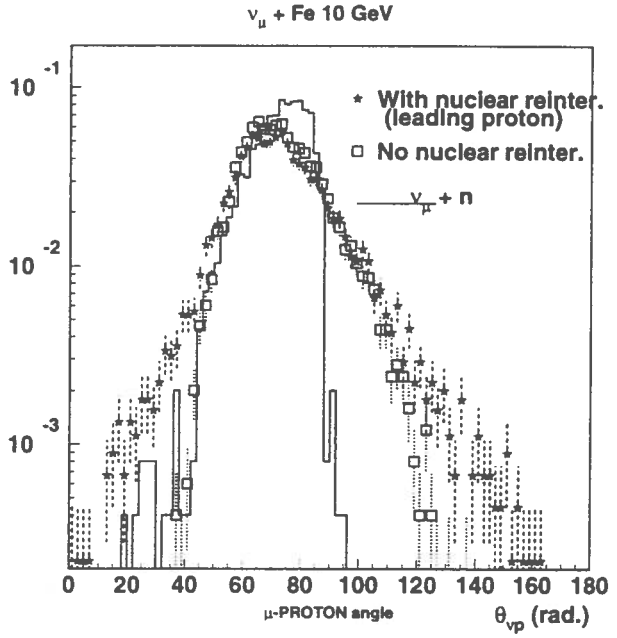

Figure 4: Distribution of the angle between the outgoing proton and the neutrino direction, in ν_μ+Fe interaction, $E_{\nu_\mu} = 10$ GeV)

This is clear in the bottom part of Fig. 5 and 6, where we show the scatter plot of the angle between the proton transverse momentum $P_\perp^p$ and the muon $P_\perp^\mu(\phi_2)$, versus the angle between $P_\perp^p$ and the missing transverse momentum $P_\perp^{miss}$ (ϕ_1). For completeness we show in Fig. 7 the case of ν_τ+n$\rightarrow\tau$+p, where we considered the channel $\tau\rightarrow\mu+\nu+\bar{\nu}$ in Fe target. Due to nuclear effects, we observe the presence of events in which ν_μ interactions give small ϕ_1 angles, close to the region expected for ν_τ candidates.

The intranuclear cascade is relevant as far as the ν_μ and ν_e are concerned, while in this last case (ν_τ,$\tau\rightarrow\mu+\nu+\bar{\nu}$) it is obscured by the missing $P_\perp$ introduced by the τ decay. In any case, it seems that, despite the smearing introduced by nuclear re-interactions, a region still exists in the ϕ_2–ϕ_1 plane which allows the identification of τ candidates. Just to consider an example, although only at particle level, if we take , the (non optimized) region on the right of the triangle drawn in the rightmost bottom plot of Fig. 7, we find that the efficiency of detecting a τ candidate is

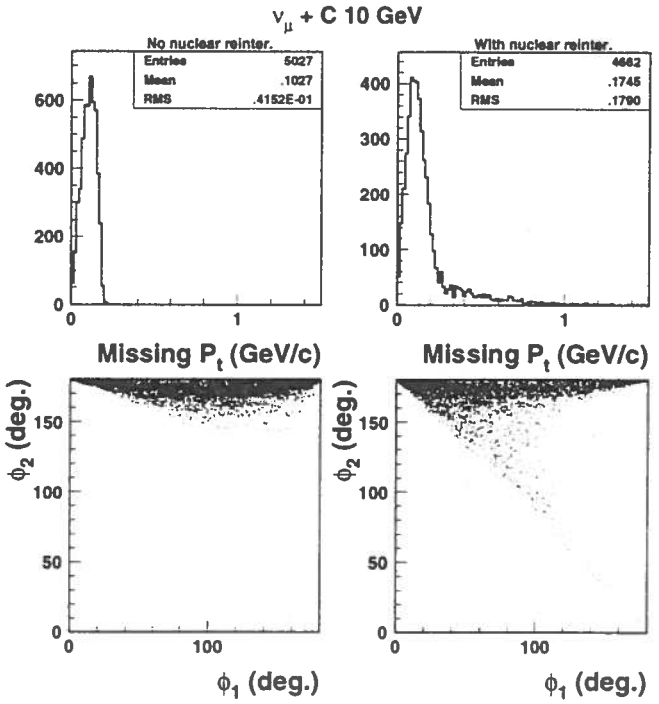

Figure 5: ν_μ+C interaction(E_{ν_μ}=10 GeV). Missing $P_\perp$ distribution (top) without (left) and with nuclear re–interaction (right). Scatter plot of ϕ_1 and ϕ_2 angles (bottom) without (left) and with (right) nuclear re–interaction.

864/4584, having rejected 100% of 4514 ν_μ interactions. Of course, this is just an over simplification, since in practice all the other resolution effects coming from a realistic experimental simulation have to be considered.

4 Delta resonance

Delta resonance process has been included in our code, for both CC and NC interactions. As a relevant example for experimental application, we have considered 5,000 CC interations of 10 GeV ν_μ on Iron. All the channels $\Delta^{++}\rightarrow p+\pi^+$, $\Delta^+\rightarrow p+\pi^0$ and $\Delta^+\rightarrow n+\pi^+$ have been considered, and the results are shown in Table 2. As in the case of QEL interaction, we see the presence of extra particles in the final state: in

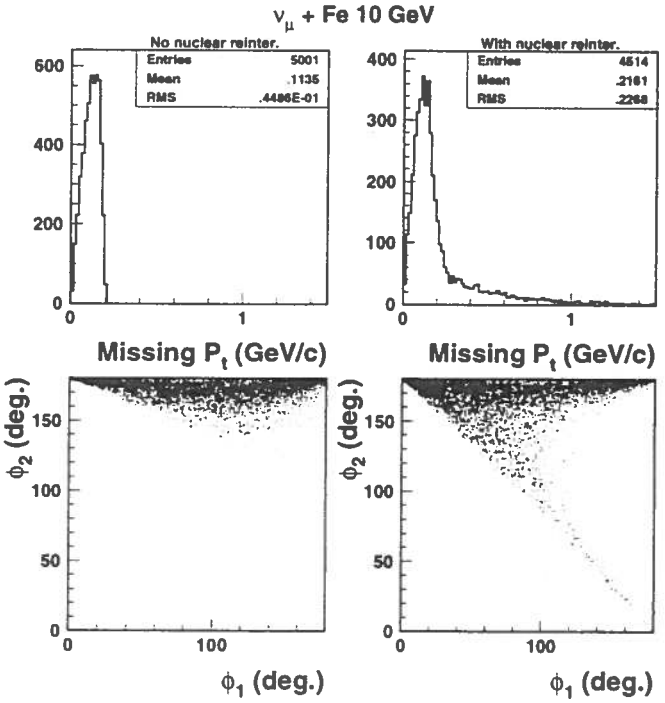

Figure 6: ν_μ+Fe interaction(E_{ν_μ}=10 GeV. Missing $P_\perp$ distribution(top) without (left) and with nuclear re–interaction (right). Scatter plot of ϕ_1 and ϕ_2 angles(bottom) without(left) and with (right) nuclear re–interaction.

practice, for Fe target, we never observe events preserving the final state obtainable without nuclear reinteractions. It might be intersting to notice how in a non negligible fraction of cases the charged pion can be absorbed inside the nucleus. This complicates the separation of quasi elastic interactions from resonance excitation: these two classes must be always considered together. Also, the effect of the nuclear rescattering manifests in an additional tail of event missing momentum.

5 Conclusions

We have shown how the nuclear re–interaction in quasi elastic neutrino events can play an important role in the experimental neutrino detection. The nuclear models

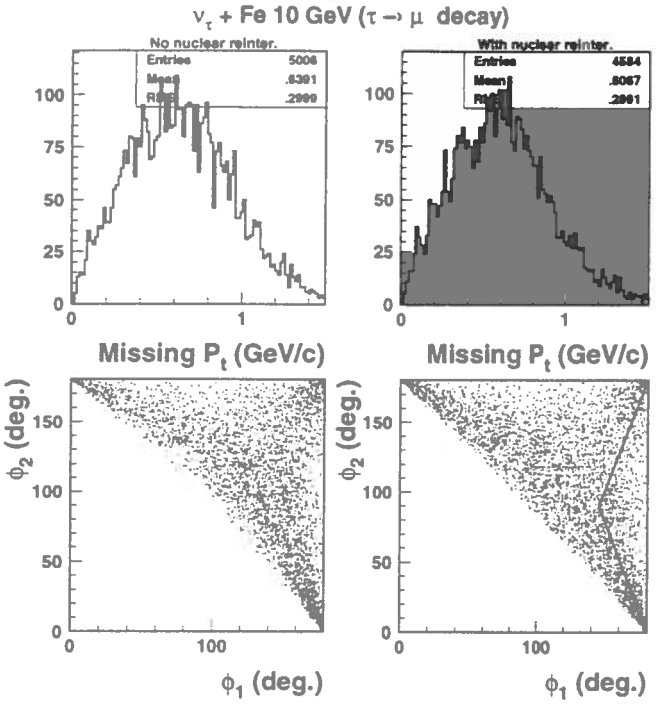

Figure 7: ν_τ+C interaction(E_{ν_μ}=10 GeV. Missing $P_\perp$ distribution(top) without (left) and with nuclear reinteraction(right). Scatter plot of ϕ_1 and ϕ_2 angles(bottom) without(left) and with (right) nuclear reinteraction. A possible selection area to identify τ candidates is the one to the right of the triangle drawn in the last plot.

contained in the DPMJET code seems to be adequate for the description of the phenomenology of neutrino interaction in view of design of future detectors for Long Base Line experiments. Of corse this is just a preliminary stage of the work. Further improvements will allow the inclusion of scattering. Nuclear effect introduces also changes in the total neutrino–nucleon cross section, as discussed in [33].

Process	$< N_p >$	$< N_n >$	$< N_{\pi^\pm} >$	$< N_{\pi^0} >$	$< N_\gamma >$
$\Delta^{++} \to p\pi^+$	2.14	1.97	0.85	0.03	3.68
$\Delta^{+} \to p\pi^0$	2.13	1.57	0.05	1.02	3.46
$\Delta^{+} \to n\pi^+$	1.64	2.65	0.91	0.04	3.39

Table 2: Comparison of the result of ν_μ interaction ($E_{\nu_\mu} = 10$ GeV) on Iron for different resonant processes

References

[1] The Kamiokande Collaboration, K. S. Hirata et al.: Phys. Lett. B280 (1992) 146

[2] The IMB Collaboration, R. Becker–Szendy, et al.: Phys. Rev. Lett. 69 (1992) 1010

[3] The Soudan2 Collaboration: Proc. 25th ICRC (Durban) 7 (1997) 77

[4] The CHOOZ Collaboration, M. Apollonio, et al. : hep-ex/9711002 (1997)

[5] The SuperKamiokande Collaboration: talk given by E. Kearns at Solar Neutrino Conference ITP, Santa Barbara, USA, Dec. 1997. Transparencies available at http://www.itp.uscb.edu/,

[6] Description of the Nomad experiment and of the adopted analysis method can be found in the reports CERN-SPSLC/91-21, 91-48. 91-53, 93/19, 94/21, 94/22, 1991 – 1994

[7] P. Lipari, M. Lusignoli and F. Sartogo: Phys. Rev. Lett. 74 (1995) 4384

[8] J. Ranft: Phys. Rev. D 51 (1995) 64

[9] J. Ranft: DPMJET–II, a Dual Parton Model event generator for hadron–hadron, hadron–nucleus and nucleus–nucleus collisions, Proceedings of the second SARE workshop at CERN, 1995, ed. by G.R.Stevenson, CERN/TIS–RP/977–05, p. 144, 1997

[10] J. Ranft: DPMJET version II.3 and II.4, INFN/AE–97/45, Gran Sasso report, 1997

[11] A. Ferrari, J. Ranft, S. Roesler and P. R. Sala: Z. Phys. C70 (1996) 413

[12] A. Ferrari, J. Ranft, S. Roesler and P. R. Sala: The production of residual nuclei in peripheral high energy nucleus-nucleus interactions, Santiago US–FT /9–96, 1996

[13] A. Ferrari and P. R. Sala: A new model for hadronic interactions at intermediate energies for the FLUKA code, Proc. of the *MC93 Int. Conf. on Monte-Carlo Simulation in High-Energy and Nuclear Physics*, Tallahassee, Florida, 22-26 february (1993), (World Scientific ed. 1994), p. 277, 1994

[14] A. Fassò, A. Ferrari, J. Ranft, P. R. Sala, G. R. Stevenson and J. M. Zazula: Proc. of the workshop on *Simulating Accelerator Radiation Environment, SARE*, Santa Fè, 11-15 january (1993) (A. Palounek ed., Los Alamos LA-12835-C 1994), p. 134, 1994

[15] A. Fassò, A. Ferrari, J. Ranft and P. R. Sala: Proc. of the *IV International Conference on Calorimetry in High Energy Physics*, La Biodola (Elba), September 19-25 1993, (A. Menzione and A. Scribano eds., World Scientific 1994), p. 493., 1994

[16] A. Fassò, A. Ferrari, J. Ranft and P. R. Sala: Proceedings of the second SARE workshop at CERN, 1995, ed. by G.R.Stevenson, CERN/TIS–RP/977–05, 1997

[17] A. Ferrari and P. R. Sala: Proc. of the *Workshop on Nuclear Reaction Data and Nuclear Reactors Physics, Design and Safety*, International Centre for Theoretical Physics, Miramare–Trieste, Italy, 15 April - 17 May 1996 in press, 1996

[18] D. Cavalli, A. Ferrari, A. Rubbia and P. R. Sala: Icarus Internal note, 1997

[19] C.H. Llewellyn Smith: Phys. Rep. 3 No. 5 (1972) 261

[20] C. Albright and C. Jarlskog: Nuclear Phys. B84 (1975) 467

[21] L. Stodolsky: Formation Zone Description in Multiproduction, in Proceedings of the VIth International Colloquium on Multiparticle Reactions, Oxford, U.K., p. 577, 1975

[22] J. Ranft: Z. Phys. C43 (1989) 439

[23] K. Hänssgen and J. Ranft: Comput. Phys. Commun. 39 (1986) 37

[24] K. Hänssgen and J. Ranft: Nucl. Sci. Eng. 88 (1984) 537

[25] T.W. Armstrong, K.C. Chandler: Nucl. Sci. Eng. 49 (1972) 110

[26] P. Cloth, D. Filges, G. Sterzenbach, T.W. Armstrong, B.L. Colborn: KFA-Report, Jül-Spez-196, 1983

[27] H.-J. Möhring and J. Ranft: Z. Phys. C52 (1991) 643

[28] R. Vandenbosh and J. R. Huizenga: *Nuclear Fission* Academic Press New York 1973

[29] V. F. Weisskopf: Phys. Rev. 52 (1937) 295

[30] N. Bohr and J. A. Wheeler: Phys. Rev. 56 (1939) 426

[31] E. Fermi: Prog. Theor. Phys. 5 (1950) 1570

[32] M. Èpherre and E. Gradsztajn: J. Physique 18 (1967) 48

[33] F. Sartogo: *Interazioni di neutrini atmosferici: un modello fenomenologico e la sua applicazione per l' interpretazione dei dati ottenibili in rivelatori sotterranei,* PhD thesis University of Roma "La Sapienza" 1995